Regular Article

PHYSICAL CHEMISTRY RESEARCH
Published by the
Iranian Chemical Society
www.physchemres.org
info@physchemres.org

Phys. Chem. Res., Vol. 13, No. 2, 197-215, June 2025
DOI: 10.22036/pcr.2025.480570.2580

Computational DFT Study on Donor and Spacer Substitution in Arylamine-Based Push-Pull Molecules for Enhanced Photovoltaic Performance

M. Boutkbout Nait Moudou[a], H. EL Ouafy[a], W. Iken[a], M.R. Chriyaa[a], S. Naciri[a], L. Halil[a], M. Aamor[a], and T. EL Ouafy[b,*]

[a]*Laboratory of Engineering in Chemistry and Physics of Matter, Faculty of Sciences and Technics, Sultan Moulay Slimane University, Beni Mellal, Morocco*

[b]*Laboratory of Engineering in Chemistry and Physics of Matter, Faculty of Medicine and Pharmacy, Sultan Moulay Slimane University, Beni Mellal, Morocco*

(Received 27 September 2024, Accepted 30 January 2025)

In this research, we will shed light on four simple molecules of the "push-pull" types (DPMA-T-DCV, DPMA-Se-DCV, MeCz-T-DCV, and MeCz-Se-DCV) by investigating the impact of substituting the electron-donor block diphenylmethylamine (DPMA) by a N-methyl carbazol-3-yl group (MeCz) and replacing the thiophene π-spacer by a selenophene, while keeping the dicyanovinyl (DCV) group constant. These molecules are optimized by the DFT method at CAM-B3LYP functional level of the theory and 6-311G(d,p) basis set. Quantum chemical calculations show that these new compounds are suitable for use as electron donors in combination with acceptors such as phenyl-C61-butyric acid methyl ester (PCBM) in bulk-heterojunction solar cells for several reasons, including: i) all molecules present good optical properties and absorb in the visible zone between 507.03-587.72 nm, these values are almost similar to the experimental results 467-514 nm. ii) the energy gaps of the four investigated molecules range from 1.24 eV to 2.011 eV, which shows that all energy gaps are in good accordance with the condition to be used as a photovoltaic material. Additionally, our results indicate a significant increase in the energy gap (0.30 eV) when substituting DPMA by MeCz in the thiophene series, aligning well with experimental observations (approximately 0.27 eV).

Keywords: Density Functional Theory, Organic solar cells, Donor, Acceptor, Photoconversion yield

INTRODUCTION

Expanding the energy conversion efficiency of organic photovoltaic cells (OPVs) is a key focus in the search for sustainable solutions to the energy crisis. Currently, global energy demand exceeds supply, particularly from fossil fuels, leading to an urgent call for alternative energy sources. Solar energy is a promising alternative, as the amount of sunlight that falls on the Earth's surface in just one hour could meet global energy needs for an entire year [1,2]. Traditional silicon-based solar cells have achieved an energy conversion efficiency (PCE) of around 15% [3], but their high cost and complex manufacturing processes have driven the search for more cost-effective alternatives. Organic solar cells (OSCs) have attracted considerable attention due to their lightweight, flexible nature and low production costs [4].

Dye-sensitized solar cells (DSSCs) have also seen significant advances in efficiency and stability since their introduction in 1991 [5]. Current DSSCs typically exhibit photoconversion efficiencies exceeding 10%, with a record of 14.3% [6]. These cells offer several advantages, including low cost, eco-friendliness, and simple production processes [7-9]. Among the various strategies to enhance photovoltaic performance, the development of new push-pull type organic dyes as photosensitizers has shown great promise. Push-pull chromophores are a well-studied class of π-conjugated molecules with applications in nonlinear optics [10], organic field-effect transistors (OFETs) [11], organic light-emitting

*Corresponding author. E-mail: tarikelouafy@gmail.com

diodes (OLEDs) [12], OSCs [13], and DSSCs [14]. These chromophores are particularly effective in bulk heterojunction (BHJ) OSCs, where polymeric push-pull donors are blended with fullerene-derivative acceptors, such as phenyl-C61-butyric acid methyl ester (PCBM), to improve PCE. The incorporation of push-pull type (D-π-A) copolymers, which consist of an electron donor (D) and an electron acceptor (A) linked by a π-conjugated bridge, results in a low bandgap and a wide absorption range, both of which are critical for enhancing photovoltaic performance [15-18].

The BHJ architecture is a major innovation in organic solar cells [19]. It involves blending donor and acceptor materials to create a nanoscale interpenetrating network, which facilitates efficient exciton dissociation and charge carrier transport [20]. When sunlight strikes the active layer, excitons are generated and separated at the donor-acceptor interface, resulting in free charge carriers (electrons and holes) that migrate toward their respective electrodes [21]. For efficient charge transfer, suitable donor and acceptor materials are essential [22]. An ideal donor material should have a high absorption coefficient to capture sunlight efficiently, a suitable HOMO-LUMO energy alignment with the acceptor to ensure effective charge transfer, and high charge carrier mobility to facilitate charge transport and reduce recombination losses [23]. The choice of donor material significantly impacts the open-circuit voltage (Voc), short-circuit current (Jsc), and overall PCE of the solar cell [24]. These factors are crucial in designing efficient donor materials for BHJ OSCs [25].

In recent decades, triarylamine derivatives (TAAs) have become prominent materials for electron donor components due to their robust electron-donating properties and high hole mobility. An early example is TPA(-T-DCV)$_3$, introduced in 2006 [26], which featured a central triphenylamine (TPA) functionalized with three thienyl (T)-DCV branches. This structure was simplified in subsequent years to create TPA-T-DCV, initially used in bi-layer OSCs with fullerene C60, resulting in an enhanced PCE of 2.5% [27,28]. Further improvements were achieved by fabricating solution-processed BHJ OSCs with PCBM, leading to a PCE of 3.0% [29]. Despite these advancements, TPA-T-DCV showed a limitation in hole mobility, as assessed by the Space Charge Limited Current (SCLC) method ($\mu_h = 1 \times 10^{-5}$ cm^2 V^{-1} s^{-1}). Various strategies were explored to enhance hole transport properties, including modifying the TPA block to improve energetics, charge transport, and photovoltaic performance. For instance, substituting one of the outer phenyl groups in the TPA unit with a methyl group resulted in the creation of DPMA-T-DCV, which exhibited a hole mobility of 5×10^{-4} cm^2 V^{-1} s^{-1}, 50 times higher than that of TPA-T-DCV. This improvement led to a higher PCE of 3.3%, compared to 2.5% for TPA-T-DCV [30].

Another strategy involved the initial rigidification of the DPMA electron-donating group using a covalent bridge, resulting in the creation of a 9-methylcarbazole moiety (MeCz) and yielding the novel push-pull molecule MeCz-T-DCV. Carbazole and its derivatives have found widespread use as hole-transporting materials in DSSCs and hybrid perovskite solar cells [31,32], as well as in host materials and emitters [33,34]. Carbazole is known for its excellent hole-transporting capabilities [35], and its HOMO level is generally slightly lower than that of triphenylamine-based donors [36,37], suggesting the potential for a higher Voc in corresponding OSCs. Moreover, substituting thiophene with selenophene in π-conjugated oligothiophenes induces a bathochromic shift in the UV-vis spectrum [38]. Selenophene-based π-conjugated systems have shown superior performance in OSCs compared to their thiophene counterparts [39]. The use of the selenophene analog of TPA-T-DCV as a donor in BHJ OSCs with PCBM resulted in a slightly higher PCE of 3.3%, compared to 3.0% for the thiophene derivative [36].

In this context, we have studied four simple push-pull compounds: DPMA-T-DCV, DPMA-Se-DCV, MeCz-T-DCV, and MeCz-Se-DCV, based on an electron-rich diphenylmethylamine (DPMA) or 9-methylcarbazole (MeCz) group (D) linked to an acceptor dicyanovinyl (DCV) group (A) via two different spacers (π), namely thiophene or selenophene. These compounds have been studied theoretically using density functional theory (DFT) at the CAM-B3LYP functional level with a 6-311G(d,p) basis set. Our objective is to explore the impact of substituting the DPMA donor group with 9-methylcarbazole (MeCz) and replacing the thiophene spacer in DPMA-T-DCV and MeCz-T-DCV with selenophene, on the parameters that affect photovoltaic performance. This study aims to identify a new donor polymer for high-performance OPV BHJ cells.

The studied molecules have been synthesized by Hossein Habibi and Pierre Josse [40] as described in Scheme 1. The DPMA-T-DCV has been prepared with a 95% yield through a direct heteroarylation reaction between 4-bromo-N-methyl-N-phenylaniline (compound 1) and thiophene-2-carbaldehyde. This reaction produced intermediate 2, which then underwent a Knoevenagel condensation with malononitrile to form the final product. While the DPMA-Se-DCV was synthesized with a 96% yield, the process began with a Stille cross-coupling reaction in toluene between compound 1 and the tributyl(selenophen-2-yl)stannane, using $Pd(PPh_3)_4$ as the catalyst. This reaction yielded compound 3 with a 50% yield. A subsequent Vilsmeier reaction selectively formed carboxaldehyde 4 with a 55% yield. Finally, DPMA-Se-DCV was synthesized through a Knoevenagel condensation of malononitrile with compound 4. Furthermore, the synthesis of the carbazole derivatives MeCz-T-DCV and MeCz-Se-DCV employed 3-bromo-9-methyl-9H-carbazole 5 as the starting material. A direct heteroarylation between compound 5 and thiophene-2-carbaldehyde yielded intermediate aldehyde 6, which underwent Knoevenagel condensation with malononitrile to produce MeCz-T-DCV with a 60% yield. In contrast, MeCz-Se-DCV was synthesized with a 94% yield through Stille cross-coupling of compound 5 with tributyl(selenophen-2-yl)stannane, resulting in compound 7 with a 45% yield. Compound 7 was then formylated to generate aldehyde 8, which underwent Knoevenagel condensation with malononitrile, ultimately yielding MeCz-Se-DCV.

COMPUTATIONAL METHODS

In this study, density functional theory (DFT) was employed to comprehensively investigate the electronic and optical properties of the target molecules. To ensure accurate and reliable theoretical predictions, a diverse set of functionals was utilized, including B3LYP [41], CAM-B3LYP [42], B3PW91 [43], WB97XD [44], and MPW1PW91 [45]. Geometry optimizations were performed using the 6-311G(d,p) basis set to achieve well-defined molecular structures, while solvent effects were incorporated using the Polarizable Continuum Model (PCM) [46] with

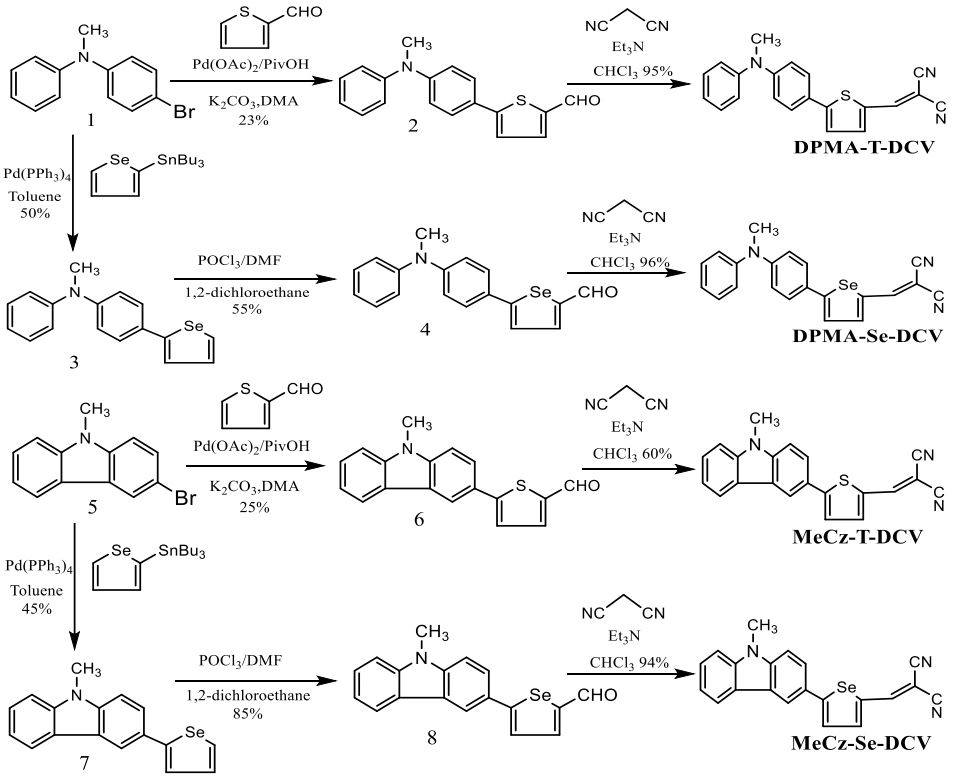

Scheme 1. Synthesis of the four studied molecules of the "push-pull" types

dichloromethane (CH_2Cl_2) to maintain consistency with experimental conditions [40]. This approach provided a realistic assessment of solvent influence on molecular properties, aligning theoretical results with experimental data to enhance the reliability and relevance of the findings.

Calculations were carried out using Gaussian 09 software [47], and molecular structures and properties were visualized through GaussView 5.0.8. Additionally, time-dependent density functional theory (TD-DFT) [48] calculations were conducted to analyze the excited-state properties of the studied molecules. The same functionals and 6-311G(d,p) basis set were employed for TD-DFT calculations, ensuring methodological consistency across all computational procedures. By integrating solvent effects through the PCM model, these calculations offered a comprehensive understanding of the optical behavior of the target molecules under experimental-like conditions.

The comparison of calculated wavelengths for the target molecules using various functionals is illustrated in Fig. 1. For DPMA-T-DCV, the computed wavelengths are 832.34 nm, 568.15 nm, 813.75 nm, 723.21 nm, and 640.54 nm for B3LYP, CAM-B3LYP, B3PW91, WB97XD, and MPW1PW91, respectively, while the experimental wavelength is 498 nm. Similarly, for DPMA-Se-DCV, the calculated wavelengths are 902.98 nm, 587.72 nm, 867.16 nm, 784.82 nm, and 693.41 nm, with an experimental wavelength of 514 nm. For MeCz-T-DCV, the calculated values are 802.41 nm, 507.03 nm, 789.37 nm, 722.59 nm, and 634.07 nm, compared to the experimental wavelength of 467 nm. Lastly, for MeCz-Se-DCV, the computed values are 791.12 nm, 516.82 nm, 773.65 nm, 715.05 nm, and 604.74 nm, while the experimental wavelength is 480 nm. Among the tested functionals, CAM-B3LYP consistently provides results closest to the experimental values for all the studied molecules. Consequently, CAM-B3LYP was selected for the entire study, ensuring consistency and accuracy in the investigation of all molecular properties.

THEORETICAL METHODOLOGY

The highest occupied molecular orbital (HOMO) and the lowest unoccupied molecular orbital (LUMO) analyses were conducted to elucidate the molecular characteristics of the studied molecules. The chemical hardness, chemical potential, softness, and electrophilicity index of the four molecules were estimated based on the frontier molecular orbital sizes to provide further insights into their molecular properties [49-55]:

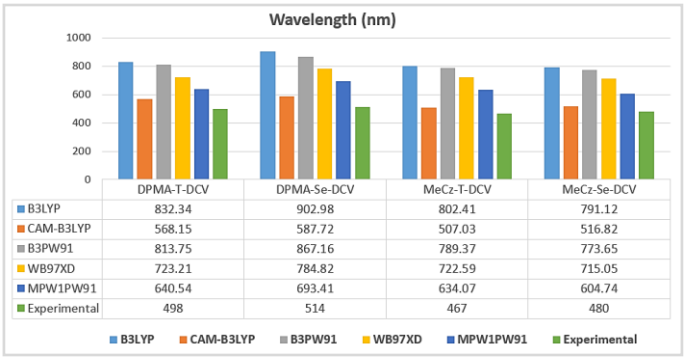

	DPMA-T-DCV	DPMA-Se-DCV	MeCz-T-DCV	MeCz-Se-DCV
B3LYP	832.34	902.98	802.41	791.12
CAM-B3LYP	568.15	587.72	507.03	516.82
B3PW91	813.75	867.16	789.37	773.65
WB97XD	723.21	784.82	722.59	715.05
MPW1PW91	640.54	693.41	634.07	604.74
Experimental	498	514	467	480

Fig. 1. Comparison of experimental and calculated wavelengths for target molecules using various functionals with the 6-311G(d,p) basis set.

$$\mu = \frac{(E_{HOMO} + E_{LUMO})}{2} \quad (1)$$

$$\eta = -\frac{(E_{HOMO} - E_{LUMO})}{2} \quad (2)$$

$$S = \frac{1}{2\eta} \quad (3)$$

$$\omega = \frac{\mu^2}{2\eta} \quad (4)$$

where μ, η, S, and ω are successively chemical potential, global hardness, chemical softness, and global electrophilicity in eV, E_{HOMO} and E_{LUMO} are the HOMO and LUMO energy of compounds in eV, respectively.

RESULT AND DISCUSSION

In this paper, we investigate the frontier molecular orbitals (FMO), molecular electrostatic potential (MEP), nonlinear optical (NLO) properties, global reactivity descriptors, as well as the electronic, optical, and photovoltaic properties of the four developed compounds.

Optimized Structures

The optimized and labeled structures of the four molecules were investigated using CAM-B3LYP/ 6-311G(d,p) as shown in Fig. 2.

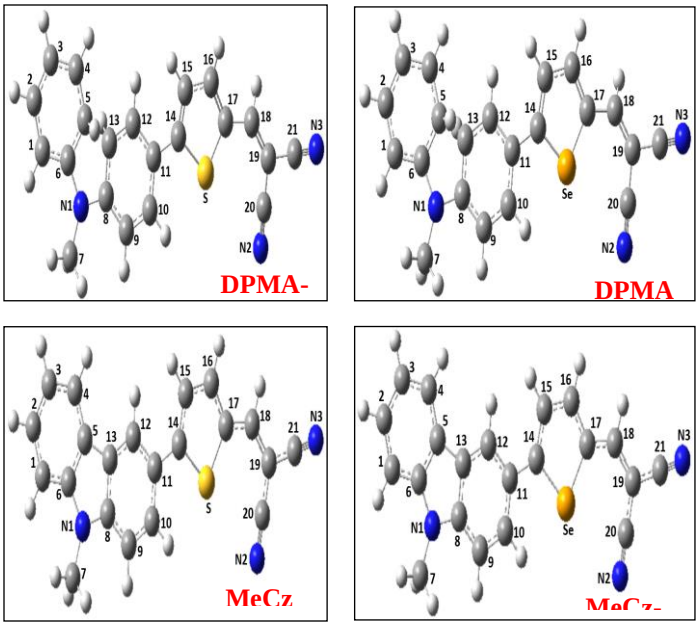

Fig. 2. Optimized and labeled structures of the four studied molecules. The blue color stands for nitrogen, the yellow for sulfur, the orange for selenium, the dark gray for carbon, and the white for hydrogen atoms.

The optimized geometrical parameters of the four studied molecules calculated by CAM-B3LYP level with the 6-311G(d,p) basis set are listed in Tables 1, 2 and 3.

From Table 1, the calculated optimized lengths of the carbon-carbon (C-C) bonds in the four studied molecules range from 1.380 to 1.449 Å. Additionally, it is noted that the sulfur-carbon (S-C) and selenium-carbon (Se-C) bonds are the longest among the studied molecules. The S-C bond lengths range from 1.8154 to 1.8244 Å for thiophene-based compounds, while the Se-C bond lengths range from 1.9175 to 1.9268 Å for selenophene-based compounds. On the other hand, the bond lengths of the N≡C cyanogen group are the shortest, varying between 1.1756 and 1.1763 Å.

In addition, the bond angles calculated using the CAM-B3LYP/6-311G(d,p) method are reported in Table 2. It is mentioned that the bond angles C6-N1-C7, C6-N1-C8, C12-C11-C14, and C20-C19-C21 are slightly smaller than 125°, while C11-C14-C15 and C17-C18-C19 are slightly larger than 125°.

Furthermore, Table 3 shows that the compounds DPMA-Se-DCV and MeCz-Se-DCV are described as nearly planar, with slight torsion angles between the planar D (donor) and π-A (acceptor) moieties. The specific dihedral angles mentioned are Se-C14-C11-C10 = 4.163° and C15-C14-C11-C12 = 4.462° for DPMA-Se-DCV, and Se-C14-C11-C10 = -0.249° and C15-C14-C11-C12 = -0.123° for MeCz-Se-DCV.

Table 1. The Bond Lengths in Angstrom (Å) were Obtained by CAM-B3LYP/6-311G(d,p)

d (Å)	DPMA-T-DCV	DPMA-Se-DCV	MeCz-T-DCV	MeCz-Se-DCV	d (Å)	DPMA-T-DCV	DPMA-Se-DCV	MeCz-T-DCV	MeCz-Se-DCV
d C1-C2	1.39848	1.39852	1.39783	1.39788	**d C13-C8**	1.41948	1.41929	1.42874	1.42830
d C2-C3	1.39964	1.39965	1.40860	1.40854	**d C11-C14**	1.44993	1.44793	1.45575	1.45365
d C3-C4	1.40054	1.40055	1.39679	1.39684	**d C14-S,Se**	1.81749	1.91676	1.81545	1.91578
d C4-C5	1.39792	1.39789	1.40054	1.40039	**d S,Se-C17**	1.82445	1.92684	1.82351	1.92534
d C5-C6	1.40556	1.43609	1.42413	1.42409	**d C17-C16**	1.39169	1.39263	1.41928	1.39170
d C6-N1	1.43605	1.47094	1.40342	1.40369	**d C16-C15**	1.40852	1.40746	1.37883	1.40847
d N1-C7	1.47100	1.47008	1.45560	1.45555	**d C15-C14**	1.38906	1.38884	1.42640	1.38733
d N1-C8	1.39399	1.39404	1.39138	1.39120	**d C17-C18**	1.81749	1.41452	1.41928	1.41586
d C8-C9	1.41690	1.41693	1.40087	1.40089	**d C18-C19**	1.38009	1.38118	1.37883	1.38009
d C9-C10	1.38894	1.38834	1.39040	1.38966	**d C19-C20**	1.42601	1.42510	1.42640	1.42541
d C10-C11	1.41181	1.41152	1.42187	1.42195	**d C20-N2**	1.17610	1.17655	1.17591	1.17638
d C11-C12	1.41727	1.41674	1.41202	1.41183	**d C19-C21**	1.42891	1.42746	1.42929	1.42777
d C12-C13	1.38521	1.38519	1.39271	1.39214	**d C21-N3**	1.17584	1.17596	1.17564	1.17578

Table 2. The Bond Angles in Degrees (°) were Obtained by CAM-B3LYP/6-311G(d,p)

Products	C6-N1-C7	C6-N1-C8	C12-C11-C14	C11-C14-C15	C17-C18-C19	C20-C19-C21
DPMA-T-DCV	117.9305	122.1853	121.0014	129.0374	130.9791	116.7031
DPMA-Se-DCV	117.9121	122.2349	121.6408	127.9723	130.4766	117.1349
MeCz-T-DCV	125.1303	108.8152	120.0517	128.8670	130.9311	116.6885
MeCz-Se-DCV	125.1442	108.8071	120.7603	127.8838	130.4565	117.1268

Table 3. The Dihedral Angles were Obtained by CAM-B3LYP/6-311G(d,p)

Product	S,Se-C14-C11-C10	C15-C14-C11-C10	C15-C14-C11-C12
DPMA-T-DCV	10.2658	-169.9785	10.3554
DPMA-Se-DCV	4.1633	-175.6160	4.4623
MeCz-T-DCV	17.3379	-163.0194	17.1645
MeCz-Se-DCV	-0.2493	179.7437	-0.1230

In contrast, the compounds DPMA-T-DCV and MeCz-T-DCV are described as less planar, with higher dihedral angles: S-C14-C11-C10 = 10.266° and C15-C14-C11-C12 = 10.355° for DPMA-T-DCV, and S-C14-C11-C10 = 17.338° and C15-C14-C11-C12 = 17.16457° for MeCz-T-DCV.

Frontier Molecular Orbitals (FMOs)

The major factor which can impact the photocurrent of any material is the energy gap of the material. The material's small band gap enables efficient electron transport from the ground state to the excited state when it absorbs light at a specific wavelength, in accordance with band theory. It is famous that functional photovoltaic molecules operate in the interval between 0.7 eV and 2.5 eV [56]. Table 4 shows that the energy gap of the four investigated molecules ranges from 1.24 eV to 2.011 eV, which shows that all energy gaps are in very good accordance with the condition to be used as a photovoltaic material. Furthermore, our theoretical results obtained by CAM-B3LYP/6-311G(d,p) in dichloromethane (CH_2Cl_2) and experimental results [40] show that changing DPMA to MeCz in the thiophene series leads to an increase in the energy gap by approximately 0.30 eV and 0.27 eV, respectively.

Furthermore, Table 4 presents both the theoretical and experimental results for the HOMO and LUMO energy values. Notably, we observe a consistent similarity between the theoretical and experimental results when substituting the donor DPMA with MeCz. Our findings reveal that compounds based on MeCz, incorporating a methylated carbazole moiety, exhibit higher LUMO energies compared to DPMA-based compounds. Specifically, in the thiophene series, the increase is approximately 0.117 eV, while in the selenophene series, it rises to 0.379 eV. This discrepancy is attributed to the presence of the methyl group in MeCz-based compounds. Conversely, DPMA-based compounds demonstrate higher HOMO values compared to MeCz-based compounds, with a difference of approximately 0.185 eV in the thiophene series and 0.372 eV in the selenophene series, this implies that DPMA-based compounds possess a higher electron density in their highest occupied orbital, indicating an elevated electron-donating capacity. Consequently, these compounds can effectively serve as efficient electron donors in solar cells. Notably, all four molecules investigated possess HOMO energy levels higher than that of the acceptor material, PCBM. This energy alignment allows efficient electron transfer from the donor molecules to PCBM, facilitating charge separation and current generation in solar cells.

Moreover, the efficiency of exciton dissociation in organic photovoltaic cells is critically influenced by the

Table 4. Theoretical and Experimental Analysis of HOMO Energy, LUMO Energy, Energy Gap, Chemical Potential, Global Hardness, Softness, and Global Electrophilicity for all Compounds

Products	$E_{HOMO}(ev)$[a]	$E_{LUMO}(ev)$[a]	$E_{gap}(ev)$[a]	$E_{HOMO}(ev)$[b]	$E_{LUMO}(ev)$[b]	$E_{gap}(ev)$[b]	$\mu(ev)$[a]	$\eta(ev)$[a]	$S(ev)$[a]	$w(ev)$[a]
DPMA-T-DCV	-5.801	-4.561	1.240	-5.56	-3.64	1.92	-5.181	0.620	0.806	21.647
DPMA-SE-DCV	-5.708	-4.448	1.260	-	-	-	-5.078	0.630	0.794	21.304
MECZ-T-DCV	-5.986	-4.4436	1.542	-5.80	-3.62	2.18	-5.215	0.771	0.649	17.637
MECZ-SE-DCV	-6.080	-4.069	2.011	-	-	-	-5.074	1.005	0.498	12.809
PCBM	-6.110	-3.711	2.399	-	-	-	-4.910	1.199	0.417	10.053

[a]Using CAM-B3LYP/6-311G(d,p) in CH_2Cl_2. [b]Using cyclic voltammetry with a 1 mM solution of the compound dissolved in dichloromethane in the presence of 0.10 M Bu_4NPF_6.

energy difference between the LUMO levels of the donor and acceptor materials. A minimum ΔE_{LUMO} of 0.3 eV is generally required to ensure effective charge separation and exciton dissociation [57,58]. All the studied molecules satisfy this requirement, highlighting their potential for efficient charge transfer. Specifically, the ΔE_{LUMO} values relative to PCBM are 0.85 eV, 0.74 eV, 0.73 eV, and 0.36 eV for DPMA-T-DCV, DPMA-Se-DCV, MeCz-T-DCV, and MeCz-Se-DCV, respectively. These findings reveal distinct trends. DPMA-based compounds exhibit higher ΔE_{LUMO} values, indicating a stronger driving force for exciton dissociation. This pronounced energy offset likely facilitates rapid and efficient charge transfer, minimizing recombination losses. In contrast, the MeCz-based molecules show comparatively lower ΔE_{LUMO} values, with MeCz-Se-DCV nearing the lower threshold. Despite this, the MeCz-based compounds benefit from additional favorable molecular interactions and electronic properties, which appear to compensate for their relatively modest driving forces, contributing to competitive photovoltaic performance.

These results highlight the critical role of balancing energy alignment and driving force efficiency through electronic structure optimization and molecular design. By tailoring donor and spacer groups, it is possible to fine-tune Δ_{ELUMO} and enhance overall device performance, demonstrating the significance of strategic molecular engineering in photovoltaic research.

Furthermore, the charge distribution of the molecular orbital of an organic molecule is so important to know its electronic behavior, especially the charge separation between occupied and virtual orbitals to provide a reasonable qualitative signal throughout the excitation process. The electron density distribution in HOMO and LUMO of the four molecules studied is exposed in Fig. 3. We notice the electron distributions of HOMOs are hugely concentrated on the conjugation spacer groups and the electron donor fragments, this indicates that these regions have a higher electron density and are more likely to donate electrons. Whereas, the electron distributions of LUMOs are concentrated on the electron acceptor units (DCV), this implies that these regions have a lower electron density and are more likely to accept electrons. Based on these observations, it can be inferred that the electron transport within these compounds occurs from the electron-rich regions (DPMA and MeCz) to the electron-poor region (DCV). This movement of electrons from the HOMO to the LUMO is often associated with intramolecular charge transfer (ICT) processes.

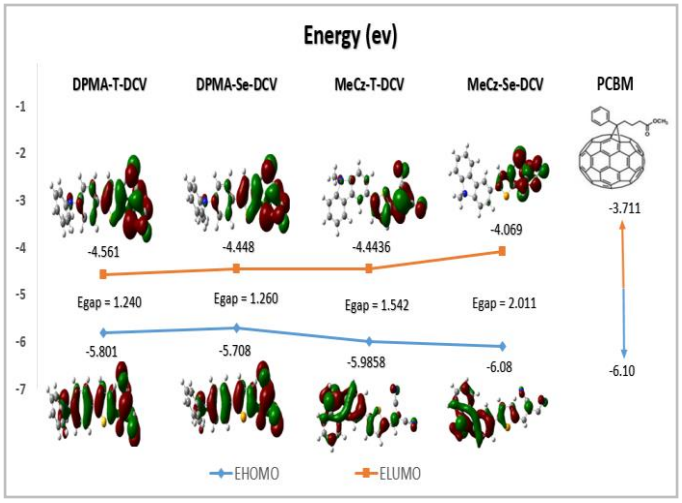

Figure 3. Energy levels of the studied molecules obtained by CAM-B3LYP/6-311G(d,p).

Global Reactivity Descriptors

The electron-donating and electron-accepting capabilities of the compounds have been characterized by chemical potential (μ), global hardness (η), chemical softness (S), and electrophilicity index (ω), the values of these parameters are given in Table 4.

The electronic chemical potential determines the direction of electron transfer when two molecules undergo condensation. A smaller value of this parameter signifies greater stability in a compound [59]. As illustrated in graph (a), replacing the thiophene spacer with a selenophene spacer leads to an increase in the electronic chemical potential. Additionally, the negative chemical potential values of the molecules investigated highlight the stability of all these compounds.

Moreover, global hardness provides insight into the ability of a molecule to retain its electrons in a given environment. From curve (b), we observe that replacing the electron-donating group DPMA with MeCz and substituting the thiophene spacer with a selenophene spacer result in an increase in global hardness. This indicates that MeCz-Se-DCV retains more electrons in its environment, while DPMA-T-DCV exhibits higher reactivity compared to the other compounds. On the other hand, the PCBM compound has a higher hardness value than the other molecules, indicating that PCBM is less likely to release electrons. Conversely, the four studied molecules are better candidates for donating electrons to PCBM.

Furthermore, softness measures the ease with which the A^+ cationic molecule can accept electrons or the A^- anionic molecule can donate electrons. Curve (c) shows that replacing the electron donor group DPMA with MeCz and substituting the thiophene spacer with a selenophene spacer result in a decrease in softness. This indicates that MeCz-Se-DCV is less able to accept or donate electrons, making it less reactive than the other compounds.

In addition, the global electrophilicity index classifies the electrophilicity of the investigated compounds. As shown in curve (d), the effect of substituting the donor group and spacer is the same as for softness. The increasing order of the global electrophilicity index is as follows: MeCz-Se-DCV < MeCz-T-DCV < DPMA-Se-DCV < DPMA-T-DCV.

Molecular Electrostatic Potential (MEP)

The molecular electrostatic potential (MEP) is a crucial tool for understanding molecular interactions within a specific molecule. Additionally, it helps identify sites of relative reactivity for electrophilic and nucleophilic attacks, studies of zeolites, molecular clusters, crystal orientations, hydrogen bonding interactions, biological recognition studies, and the correlation and prediction of a wide variety of macroscopic properties [60-62].

It can be observed from Fig. 5 that the different colors represent the electrostatic potential on the surface of the molecule. The red regions correspond to areas of negative electrostatic potential, while the blue regions indicate areas of positive electrostatic potential. The green regions in the middle represent a zero electrostatic potential. Additionally, it is evident that electrophilic reactivity is associated with the negative regions (red), whereas nucleophilic reactivity is linked to the positive regions (blue). The electrostatic potential increases in the following order: red < orange < yellow < green < blue. Consequently, the thiophene or selenophene spacer is highlighted by the blue regions, and the cyanogen group of the acceptor group DCV is indicated by the red regions.

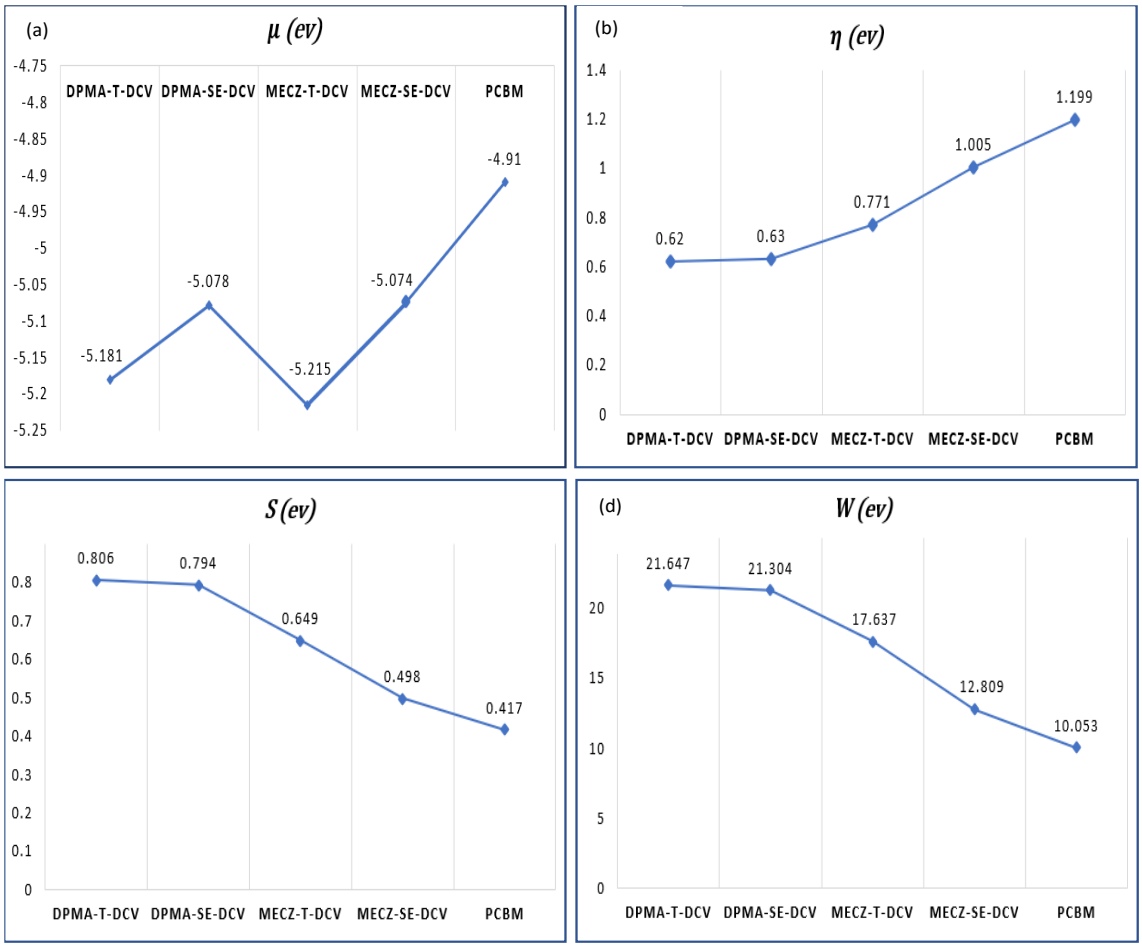

Fig. 4. (a) Chemical potential, (b) global hardness, (c) softness, and (d) global electrophilicity of all compounds.

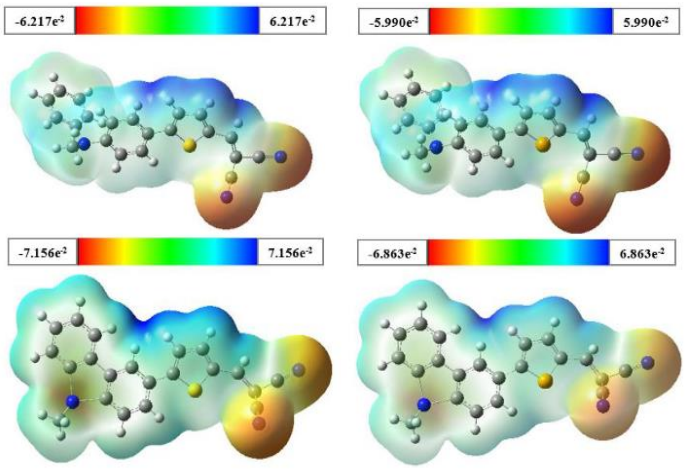

Fig. 5. Electrostatic potentials of the surface of the four push-pull molecules.

Optical Properties

Absorption plays a crucial role in determining the performance of photovoltaics. To achieve optimal efficiency, molecules must efficiently absorb light and maintain stability within the visible spectrum. The molecular orbital properties, maximum absorption wavelengths (λ_{max}), oscillator strengths (f), and excitation energies (E_{ex}) for all the studied molecules are presented in Table 6. Additionally, Fig. 6 illustrates the UV-Vis absorption spectra of the examined molecules in dichloromethane (CH_2Cl_2), calculated using the default settings of Gaussian 09 software with the CAM-B3LYP/6-311G(d,p) method.

We observe that all the molecules exhibit absorption within the visible range, specifically between 507.03 and 587.72 nm. These values closely match the experimental results, which fall within the range of 467-514 nm [40],

Table 6. Relevant Molecular Orbital Assignments, Absorption Spectrum Maxima (λ_{max}) Excitation Energy (E_{ex}), and Oscillator Strengths (f) of all Molecules

Products	λmax^a	λmax^b	f^a	Assignments (%)[a]	Eex (ev)[a]
DPMA-T-DCV	568.15	498	0.5913	H------L (15.36%)	2.1822
	412.09		0.0067	H-3-----L (15.43%)	3.0087
DPMA-Se-DCV	587.72	514	0.4763	H------L (13.46%)	2.1096
	479.15		0.0345	H-3-----L (65.75%)	2.5876
MeCz-T-DCV	507.03	467	0.7572	H------L (29.01%)	2.4453
	421.67		0.0096	H-----L+2 (62.49%)	2.9403
MeCz-Se-DCV	516.82	480	0.6865	H-1-----L (48.05%)	2.3990
	421.48		0.0101	H-----L+2 (70.75%)	2.9417

[a]Using CAM-B3LYP/6-311G(d,p) in CH_2Cl_2. [b]Using UV-Vis spectroscopy in CH_2Cl_2.

Table 7. HOMO Energy, LUMO Energy, Energy Gap, Open Circuit Voltage, Dimensionless Voltage, Fill Factor, Light-Harvesting Efficiency at λ and the Power Conversion Efficiency (η) of all Compounds

Products	E_{HOMO} (ev)	E_{LUMO} (ev)	E_{GAP} (ev)	V_{oc} (v)	υ_{oc}	FF (%)	LHE (λ)	η (%)
DPMA-T-DCV	-5.801	-4.561	1.240	1.790	69.610	92.6	0.744	13.89
DPMA-Se-DCV	-5.708	-4.448	1.260	1.697	65.993	92.2	0.660	13.11
MeCz-T-DCV	-5.986	-4.444	1.542	1.975	76.796	93.1	0.825	15.41
MeCz-Se-DCV	-6.080	-4.069	2.011	2.069	80.460	93.4	0.794	16.19
PCBM	-6.110	-3.711	2.399					

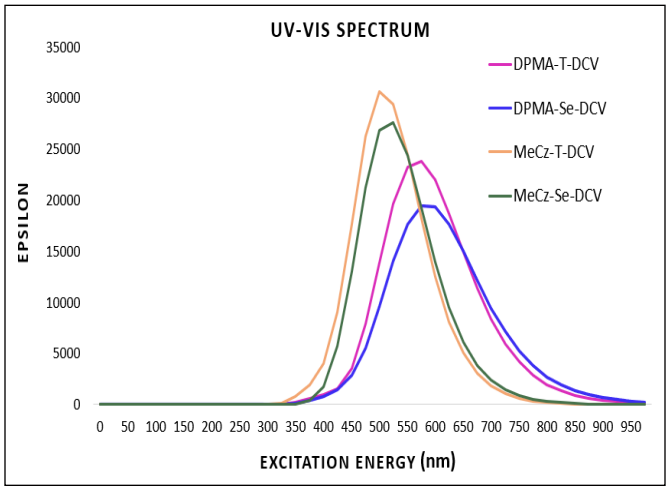

Fig. 6. UV-visible spectrum of all molecules at CAM-B3LYP/6-311G(d,p) in CH_2Cl_2.

Photovoltaic Proprieties

In this section, we discuss the photovoltaic properties related to the four studied molecules. It is noteworthy that the power conversion efficiency (η) is considered as an important parameter to verify the performance of solar cells which is estimated by determining the open circuit voltage, the fill factor, the LHE. The values of these parameters are given in Table 7.

The power conversion efficiency (η) of the solar cell is estimated using the following equation:

$$\eta = \frac{J_{sc}\, V_{oc}\, FF}{P_{in}} \qquad (5)$$

where J_{SC} represents the short-circuit current density, commonly set at 8.38 mA cm^{-2} for the fabrication and optimization of solar cells. V_{OC} refers to the open-circuit voltage, while FF denotes the fill factor. P_{in} represents the

incident light power on the solar cell during power conversion efficiency (PCE) measurements, typically set at AM 1.5G and 100 mW cm^{-2}. The open-circuit voltage (V_{OC}) is determined by the energy difference between the HOMO level of the donor and the LUMO level of the acceptor [63,64]:

$$Voc = \frac{1}{e}(|E_{HOMO}(Donor)| - |E_{LUMO}(Acceptor)| - 0{,}3) \quad (6)$$

where E_{HOMO} (Donor) is the HOMO energy of the donor, E_{LUMO} (Acceptor) is the LUMO energy of the acceptor, e represents the elementary charge, and the value of 0.3 V accounts for the loss factor associated with the heterojunction design.

The current density of short circuit J_{SC} values was estimated by the following equation:

$$J_{sc} = \int_{\lambda} LHE(\lambda)\phi_{in}\eta_{collec}d\lambda \quad (7)$$

where LHE(λ) is the light-harvesting efficiency at wavelength λ, φ_{in} is the electron injection efficiency, and η_{collec} is the electron collection efficiency [65,66].

To achieve high values of the short-circuit current (J_{SC}), high light-harvesting efficiency (LHE) is required, which can be calculated using the following equation:

$$LHE(\lambda) = 1 - 10^{-f} \quad (8)$$

where f represents the oscillator strength of the donor material, related to the maximum absorption wavelength (λ_{max}) [67,68].

Additionally, one of the most crucial factors influencing power conversion efficiency (η) is the fill factor (FF), which can be calculated using the following equation [69]:

$$FF = \frac{\nu_{oc} - ln(\nu_{oc} + 0.72)}{\nu_{oc} + 1} \quad (9)$$

where ν_{oc} is the dimensionless voltage:

$$\nu_{oc} = \frac{e\,V_{oc}}{nK_BT} \quad (10)$$

Where e, V_{OC}, K_B, T, and n represent the elementary charge of the electron, the open-circuit voltage, the Boltzmann constant, the temperature, and the ideal factor for a diode, respectively. The values of ν_{oc} were calculated with n = 1 [70].

The open circuit voltage (Voc) is a critical parameter that reflects the ability of the photovoltaic cell to generate voltage when exposed to light, and it is influenced by the recombination processes within the device. As seen in curve (a), the Voc values for the DPMA-based compounds range from 1.697 to 1.790 V, while for the MeCz-based compounds, they are higher, ranging from 1.975 to 2.069 V. This suggests that the MeCz-based compounds experience less recombination, which is beneficial for the overall device performance. A lower recombination rate typically results in higher efficiency, as the generated charge carriers are less likely to be lost, thus contributing to an increase in the power conversion efficiency (η).

The fill factor (FF) is another critical parameter that quantifies the efficiency of the photovoltaic cell by considering the shape of the current-voltage curve. A higher FF indicates that the cell can more efficiently convert the available light into electrical energy. The accuracy of Eq. (9) is particularly reliable when the dimensionless voltage (υoc) values are greater than 10. As shown in curve (b), all dimensionless voltage (υoc) values are well above 10, indicating favorable operating conditions for the devices. Furthermore, as seen in graph (c), all of the compounds exhibit a high fill factor greater than 92%, with the MeCz-based compounds displaying a superior FF compared to the DPMA-based compounds. This confirms that the MeCz-based molecules not only exhibit higher Voc values but also possess a better ability to maintain high efficiency during energy conversion, thus further supporting their enhanced power conversion efficiency (η).

In addition, the light-harvesting efficiency (LHE) plays a crucial role in determining the short-circuit current density (Jsc), which is directly related to the amount of light absorbed by the active layer. As the LHE increases, so does the Jsc, leading to a higher power conversion efficiency. This relationship is clearly outlined in Eq. (7), where an increase in LHE directly correlates with an increase in the power conversion efficiency. As seen in curve (d), the impact of changing the donor group from DPMA to MeCz has a similar effect on both Voc and FF, with the MeCz-based compounds

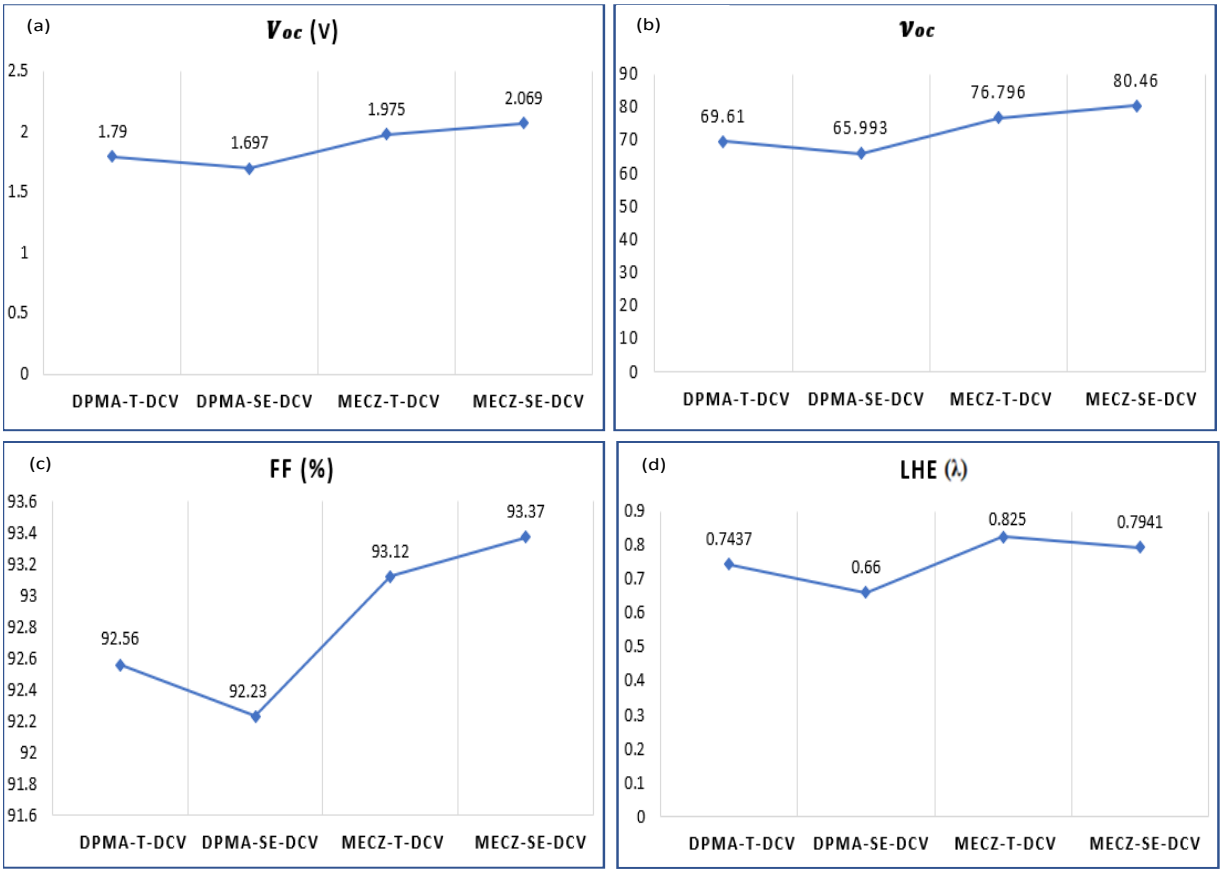

Fig. 7. (a) Open circuit voltage, (b) dimensionless voltage, (c) fill factor (d) light-harvesting efficiency at λ of all compounds.

consistently outperforming the DPMA-based ones. This further supports the conclusion that the MeCz-based compounds, due to their enhanced light absorption and reduced recombination, are more efficient in terms of power conversion efficiency, making them promising candidates for high-performance organic photovoltaic (OPV) devices.

The power conversion efficiency (PCE) of the studied molecules varies significantly based on the nature of the donor groups and spacers. As shown in Fig. 8, the DPMA-based compounds exhibit a PCE of 13.89% for DPMA-T-DCV (thiophene) and 13.11% for DPMA-Se-DCV (selenophene). In contrast, the carbazole-based compounds, MeCz-T-DCV and MeCz-Se-DCV, show higher efficiencies of 15.41% and 16.19%, respectively. This performance difference can be attributed to the nature of the donor group. The MeCz, being a stronger donor, appears to enhance the photovoltaic efficiency of the compounds, likely due to better charge injection capabilities and more favorable interactions with the DCV acceptor group. Additionally, while replacing thiophene with selenophene results in a slight decrease in PCE for the DPMA-based compounds, it has a more significant positive impact on the MeCz-based compounds, increasing their PCE substantially. These results suggest that combining MeCz with a selenophene spacer may be an effective strategy for designing high-performance materials for organic photovoltaic cells.

Nonlinear Optical (NLO)

Nonlinear optical (NLO) properties describe the capacity of a material to demonstrate effects that are nonlinearly related to the intensity of the incident light. Molecules with strong NLO characteristics can contribute significantly to solar cell efficienc y by improving ligh t harvesting,

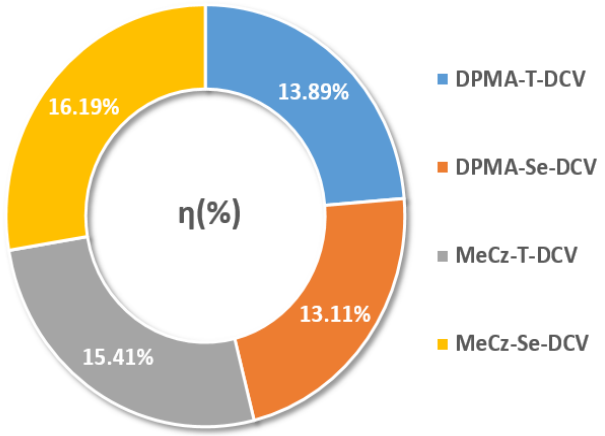

Fig. 8. Power conversion efficiency (PCE) for all studied molecules at J_{SC} 8.38. (mA cm^{-2}).

facilitating efficient exciton dissociation, and minimizing losses caused by nonradiative recombination. Optimizing the NLO properties of the selected molecules is thus crucial, as it can directly enhance photon absorption and charge transport, ultimately boosting the overall performance and energy conversion efficiency of the solar cells.

The non-linear optical (NLO) properties, including the dipole moment (DM), isotropic polarizability (α), anisotropy of the polarizability (Δα), and first-order hyperpolarizability (β_{tot}), were calculated using the following equations [71,72]:

$$DM = \sqrt{(\mu_x^2 + \mu_y^2 + \mu_z^2)} \quad (11)$$

$$\alpha = \frac{\alpha_{xx} + \alpha_{yy} + \alpha_{zz}}{3} \quad (12)$$

$$\Delta_\alpha = \sqrt{\frac{(\alpha_{xx} - \alpha_{yy})^2 + (\alpha_{yy} - \alpha_{zz})^2 + (\alpha_{zz} - \alpha_{xx})^2}{2}} \quad (13)$$

$$\beta_{tot} = \sqrt{(\beta_{xxx} + \beta_{xyy} + \beta_{xzz})^2 + (\beta_{yyy} + \beta_{xxy} + \beta_{yzz})^2 + (\beta_{zzz} + \beta_{xxz} + \beta_{zyy})^2} \quad (14)$$

where αii; β_{xxi}; β_{iyy} and β_{izz} are tensor elements of polarizability and hyperpolarizability, successively with i = x; y; z. E = 0:01 a.u was applied [73].

The dipole moment DM of the studied molecules has been calculated by the CAM-B3LYP/6-311G(d,p) method. The dipole moment has a great influence on the solubility of the molecules in different types of organic solvents and also the donor production in the self-assembly film. The results obtained in Table 8 showed that among all the four molecules, the DPMA-T-DCV molecule has the highest dipole moment, which shows that this molecule has high solubility in CH_2Cl_2, this also explains the bathochromic offset of the UV-visible spectrum of this molecule in CH_2Cl_2. And also, the DPMA-T-DCV molecule has a higher self-assembly, which will result in a higher order level at the donor-acceptor interface.

To understand the behavior and performance of a solar cell, it is essential to determine the isotropic polarizability (α), the anisotropy of the polarizability (Δα), and the total hyperpolarizability (β_{tot}) of the investigated compounds. The NLO properties provide valuable insights into the intramolecular charge delocalization within the donor electron groups [74]. Notably, large values of α, Δα, and β_{tot} indicate efficient electron mobility from the donor to the acceptor.

The values of α, Δα, and β_{tot} for the studied compounds are presented in Tables 9 and 10. The results reveal that all compounds exhibit high values of α and β_{tot}. These findings confirm the effective charge transfer from donor to acceptor, suggesting that the compounds possess strong NLO properties, which contribute positively to their photovoltaic performance. This behavior emphasizes the potential of these molecules for efficient light harvesting and electron transport in solar cell applications.

CONCLUSION

Following the work on OSCs, four new push-pull molecules were studied theoretically using quantum methods, namely density functional theory (DFT) at the CAM-B3LYP functional level of theory and the 6-311G(d,p) basis set, we studied the effect of substitution the diphenylmethylamine (DPMA) by an N-methyl carbazol-3-yl group (MeCz) or the thiophene π-spacer by a selenophene one, while keeping the dicyanovinyl (DCV) group constant. The quantum chemical calculations show that the results of the overall reactivity descriptors, energy levels, electronic, optical, photovoltaic, and NLO properties indicate that these new compounds are suitabl e for use as electron donors in

Table 8. The Dipole Moment DM of the Studied Molecules

Produits	DMx	DMy	DMz	DMTotal
DPMA-T-DCV	10.4264	-4.4159	6.2316	12.9245
DPMA-Se-DCV	9.7910	-4.4337	6.0488	12.3333
MeCz-T-DCV	11.6140	-4.2105	-0.3818	12.3596
MeCz-Se-DCV	11.0794	-4.4145	-0.3942	11.9330

Table 9. Polarizability (α) of the Four Studied Molecules

		DPMA-T-DCV	DPMA-T-DCV	DPMA-T-DCV	DPMA-T-DCV
Polarizability (α)	α_{xx}	-235.6686	-230.3252	-237.3525	-233.3378
	α_{xy}	20.5682	20.0695	8.6066	9.5768
	α_{yy}	-159.6918	-164.1082	-135.3726	-138.6772
	α_{xz}	-17.4147	-16.8731	16.9210	15.1031
	α_{yz}	-5.6838	-5.6044	-9.7540	-9.0942
	α_{zz}	-148.0502	-154.6170	-167.8532	-173.2066

Table 10. Hyperpolarizability of the Four Studied Molecules

		DPMA-T-DCV	DPMA-T-DCV	DPMA-T-DCV	DPMA-T-DCV
Hyperpolarizability (β_{total})	β_{xxx}	961.6410	765.7671	1193.0676	1029.7653
	β_{xxy}	-64.6949	-62.2181	-40.3065	-50.2959
	β_{yyz}	13.9921	11.7199	-2.5501	-4.8242
	β_{xyz}	57.4223	57.5977	58.9883	53.3028
	β_{xxz}	254.7175	255.6379	-2.5034	17.9242
	β_{yyy}	-40.6417	-41.0179	-17.2109	-7.9887
	β_{zzz}	38.8360	37.3692	-9.1334	-17.5021
	β_{xzz}	23.0894	5.7774	37.9712	11.1255
	β_{yzz}	-13.2156	-11.5779	-10.7520	-7.3899
	β_{xyy}	111.5597	75.2636	129.2797	90.6211

combination with the acceptors such as the PCBM in the bulk-heterojunction solar cell. Furthermore, all the molecules exhibit absorption within the visible range, specifically falling between 507.03 and 587.72 nm. Notably, when the thiophene spacer is replaced with selenophene, a systematic shift in the UV-visible spectrum occurs in dichloromethane. For DPMA-based compounds, this shift amounts to approximately 19.57 nm, while for MeCz-based compounds, it is around 9.79 nm. As a consequence, the increasing order of wavelengths, progressing from MeCz-T-DCV to MeCz-Se-DCV, DMPA-T-DCV, and DPMA-Se-DCV. This observed order aligns seamlessly with the experimental findings. In addition, the replacement of DPMA by MeCz causes an increase in E_{gap} values for the thiophene and selenophene series of around 0.30 ev and 0.27 ev, respectively. Moreover, compounds based on MeCz exhibit higher LUMO energies compared to DPMA-based compounds. Specifically, in the thiophene series, the increase is approximately 0.117 ev, while in the selenophene series, it rises to 0.379 ev. Conversely, DPMA-based compounds demonstrate higher HOMO values compared to MeCz-based compounds, with a difference of approximately 0.185 ev in

the thiophene series and 0.372 ev in the selenophene series. Furthermore, compounds based on MeCz demonstrate favorable photovoltaic characteristics, including open circuit voltages (Voc) of 1.975 V and 2.069 V, along with light absorption capacities (LHE) of 0.825 and 0.794 for the thiophene and selenophene series, respectively. Which implies that these molecules have the advantage of easy recombination and also an increase in short circuit current (J_{SC}) and the power conversion efficiency (η).

REFERENCES

[1] Crabtree, G. W.; Lewis. N. S., Solar energy conversion. *Phys. Today*. **2008**, *60*(3), 37-42 DOI: 10.1063/1.2718755.

[2] Barber, J., Photosynthetic energy conversion: natural and artificial. *Chem. Soc. Rev.* **2009**, *38*(1), 185-196, DOI: 10.1039/B802262N.

[3] Grätzel, M., Photoelectrochemical cells. *Nat*. **2001**, *414*(6861), 338-344, DOI: 10.1038/35104607.

[4] Guo, J.; Balakirev, D. O.; Gu, C.; Peregudova, S. M.; Ponomarenko, S. A.; Liu, Z.; Luponosov, N. Y.; Min, J.; Lei, A., End group tuning in small molecule donors for non-fullerene organic solar cells. *Dyes Pigments*. **2020**, *175*, 108078, DOI: 10.1016/j.dyepig.2019.108078

[5] O'regan, B.; Grätzel, M., A low-cost, high-efficiency solar cell based on dye-sensitized colloidal TiO_2 films. *Nat*. **1991**, *353*(6346), 737-740, DOI: 10.1038/353737a0.

[6] Kakiage, K.; Aoyama, Y.; Yano, T.; Oya, K.; Fujisawa, J. I.; Hanaya, M., Highly-efficient dye-sensitized solar cells with collaborative sensitization by silyl-anchor and carboxy-anchor dyes. *Chem. Commun*. **2015**, *51*(88), 15894-15897, DOI: 10.1039/C5CC06759F.

[7] Aboulouard, A.; Gultekin, B.; Can, M.; Erol, M.; Jouaiti, A.; Elhadadi, B.; Zafer, C.; Demic, S., Dye sensitized solar cells based on titanium dioxide nanoparticles synthesized by flame spray pyrolysis and hydrothermal sol-gel methods: a comparative study on photovoltaic performances. *J. Mater. Sci. Technol*. **2020,** *9*(2), 1569-1577, DOI: 10.1016/j.jmrt.2019.11.083.

[8] Tunç, G.; Güzel, E.; Şişman, İ.; Ahsen, V.; Cardenas-Jiron, G.; Gürek, A. G., Effect of new asymmetrical Zn (ii) phthalocyanines on the photovoltaic performance of a dye-sensitized solar cell. *New J. Chem*. **2019**, *43*(36), 14390-14401, DOI: 10.1039/C9NJ02585E.

[9] Boutkbout Nait Moudou, M.; EL Ouafy, H.; Halil, L.; Aamor, M.; Naciri, S.; Chriyaa, M. R.; Iken, W.; EL Ouafy, T., Exploring the Role of π-Spacers in Six Novel Push-Pull Photovoltaic Systems Based on N-Methylarylamine: A Theoretical DFT Investigation. *Comput. Theor. Chem.* **2025**, 1244, 115023-115035, DOI: 10.1016/j.comptc.2024.115023.

[10] Garmire, E., Nonlinear optics in daily life. *Opt. Express*. **2013**, *21*(25), 30532-30544, DOI: 10.1364/OE.21.030532

[11] Gsänger, M.; Bialas, D.; Huang, L.; Stolte, M.; Würthner, F., Organic semiconductors based on dyes and color pigments. *Adv. Mater*. **2016**, *28*(19), 3615-3645, DOI: 10.1002/adma.201505440

[12] Berner, D.; Klein, C.; Nazeeruddin, M. K.; De Angelis, F.; Castellani, M.; Bugnon, P.; Scopelliti, R.; Zuppiroli,L.; Graetzel, M., Efficient blue light-emitting diodes based on a classical "push–pull" architecture molecule 4, 4′-di-(2-(2,5-dimethoxyphenyl) ethenyl)-2, 2′-bipyridine. *J. Mater. Chem.* **2006**, *16*(46), 4468-4474, DOI: 10.1039/B610880F.

[13] Kundu, S.; Patra, A., Nanoscale strategies for light harvesting. *Chem. Rev*. **2017**, *117*(2), 712-757, DOI: 10.1021/acs.chemrev.6b00036.

[14] Higashino, T.; Imahori, H., Porphyrins as excellent dyes for dye-sensitized solar cells: recent developments and insights. *Dalton Trans*. **2015**, *44*(2), 448-463, DOI: 10.1039/C4DT02756F.

[15] Duan, C.; Huang, F.; Cao, Y., Recent development of push–pull conjugated polymers for bulk-heterojunction photovoltaics: rational design and fine tailoring of molecular structures. *J. Mater. Chem*. **2012**, *22*(21), 10416-10434, DOI: 10.1039/C2JM30470H.

[16] Hirade, M.; Yasuda, T.; Adachi, C., Effects of intramolecular donor-acceptor interactions on bimolecular recombination in small-molecule organic photovoltaic cells. *J. Phys. Chem. C*. **2013**, *117*(10), 4986-4991, DOI: 10.1021/jp400386q.

[17] Ko, H. M.; Choi, H.; Paek, S.; Kim, K.; Song, K.; Lee, J. K.; Ko, J., Molecular engineering of push-pull chromophore for efficient bulk-heterojunction morphology in solution processed small molecule organic photovoltaics. *J. Mater. Chem*. **2011**, *21*(20),

7248-7253, DOI: 10.1039/C1JM10667H.

[18] Bürckstümmer, H.; Tulyakova, E. V.; Deppisch, M.; Lenze, M. R.; Kronenberg, N. M.; Gsänger, M.; Stolte, M.; Meerholz, K.; Würthner, F., Efficient solution-processed bulk heterojunction solar cells by antiparallel supramolecular arrangement of dipolar donor-acceptor dyes. *Angew. Chem.* **2011**, *123*(49), 11832-11836, DOI: 10.1002/anie.201105133.

[19] Sharma, A.; Pathak, D.; Sharma, D. P.; Nunzi, J. M., Recent Advances in Bulk-Heterojunction Solar Cells: A Review. *Eur. Phys. J. Appl. Phys.* **2022**, *97*, 81, DOI: 10.1051/epjap/2022220113.

[20] Wadsworth, A.; Hamid, Z.; Kosco, J.; Gasparini, N.; McCulloch, I., The Bulk Heterojunction in Organic Photovoltaic, Photodetector, and Photocatalytic Applications. *Adv. Mater.* **2020**, *32*(38), 2001763, DOI: 10.1002/adma.202001763.

[21] Scharber, M. C.; Sariciftci, N. S., Efficiency of Bulk-Heterojunction Organic Solar Cells. *Prog. Polym. Sci.* **2013**, *38*(12), 1929-1940, DOI: 10.1016/j.progpolymsci.2013.05.001.

[22] Zhang, G.; Zhao, J.; Chow, P. C.; Jiang, K.; Zhang, J.; Zhu, Z.; Yan, H., Nonfullerene Acceptor Molecules for Bulk Heterojunction Organic Solar Cells. *Chem. Rev.* **2018**, *118*(7), 3447-3507, DOI: 10.1021/ acs.chemrev.7b00535.

[23] Li, Y.; Huang, W.; Zhao, D.; Wang, L.; Jiao, Z.; Huang, Q.; Yuan, G., Recent Progress in Organic Solar Cells: A Review on Materials from Acceptor to Donor. *Molecules.* **2022**, *27*(6), 1800, DOI: 10.3390/molecules27061800.

[24] Cao, J.; Yi, L.; Zhang, L.; Zou, Y.; Ding, L., Wide-bandgap polymer donors for non-fullerene organic solar cells. *J. Mater. Chem. A* **2023**, *11*(1), 17-30, DOI: 10.1039/D2TA07463J.

[25] Sun, Y.; Welch, G. C.; Leong, W. L.; Takacs, C. J.; Bazan, G. C.; Heeger, A. J., Solution-processed small-molecule solar cells with 6.7% efficiency. *Nat. Mater.* **2012**, *11* (1), 44-48, DOI: 10.1038/nmat3160.

[26] Roquet, S.; Cravino, A.; Leriche, P.; Alévêque, O.; Frere, P.; Roncali, J., Triphenylamine− thienylenevinylene Hybrid Systems with Internal Charge Transfer as Donor Materials for Heterojunction Solar Cells. *J. Am. Chem. Soc*. **2006**, *128*(10), 3459-3466, DOI: 10.1021/ja058178e.

[27] Leliège, A.; Le Regent, C. H.; Allain, M.; Blanchard, P.; Roncali, J., Structural Modulation of Internal Charge Transfer in Small Molecular Donors for Organic Solar Cells. *Chem. Commun*. **2012**, *48*(71), 8907-8909, DOI: 10.1039/C2CC33921H.

[28] Leliège, A.; Grolleau, J.; Allain, M.; Blanchard, P.; Demeter, D.; Rousseau, T.; Roncali, J., Small D–π–A Systems with o-Phenylene-Bridged Accepting Units as Active Materials for Organic Photovoltaics. *Chem. Eur. J.* **2013**, *19*(30), 9948-9960, DOI: 10.1002/chem.201301054.

[29] Labrunie, A.; Jiang, Y.; Baert, F.; Leliège, A.; Roncali, J.; Cabanetos, C.; Blanchard, P., Small Molecular Push–Pull Donors for Organic Photovoltaics: Effect of the Heterocyclic π-Spacer. *RSC Adv*. **2015**, *5*(124), 102550-102554, DOI: 10.1039/C5RA21958B.

[30] Jiang, Y.; Cabanetos, C.; Allain, M.; Liu, P.; Roncali, J., Manipulation of the Band Gap and Efficiency of a Minimalist Push–Pull Molecular Donor for Organic Solar Cells. *J. Mater. Chem. C.* **2015**, *3*(20), 5145-5151, DOI: 10.1039/C5TC00913H.

[31] Michaleviciute, A.; Degbia, M.; Tomkeviciene, A.; Schmaltz, B.; Gurskyte, E.; Grazulevicius, J. V.; Bouclé, J.; Tran-Van, F., Star-Shaped Carbazole Derivative Based Efficient Solid-State Dye Sensitized Solar Cell. *J. Power Sources.* **2014**, *253*, 230-238, DOI: 10.1016/j.jpowsour.2013.12.039.

[32] Nakar, R.; Ramos, F. J.; Dalinot, C.; Marques, P. S.; Cabanetos, C.; Leriche, P.; Sanguinet, L.; Kobeissi, M.; Blanchard, P.; Faure-Vincent, J.; Tran-Van, F., Cyclopentadithiophene and Fluorene Spiro-Core-Based Hole-Transporting Materials for Perovskite Solar Cells. *J. Phys. Chem. C*. **2019**, *123*(37), 22767-22774, DOI: 10.1021/acs.jpcc.9b05931.

[33] Wex, B.; Kaafarani, B. R., Perspective on Carbazole-Based Organic Compounds as Emitters and Hosts in TADF Applications. *J. Mater. Chem. C*. **2017**, *5*(34), 8622-8653, DOI: 10.1039/C7TC02156A.

[34] Moonsin, P.; Prachumrak, N.; Rattanawan, R.; Keawin, T.; Jungsuttiwong, S.; Sudyoadsuk, T.; Promarak, V., Carbazole Dendronised Triphenylamines as Solution Processed High Tg Amorphous Hole-Transporting

Materials for Organic Electroluminescent Devices. *Chem. Commun*. **2012**, *48*(28), 3382-3384, DOI: 10.1039/C2CC16878B.

[35] Nishimoto, T.; Yasuda, T.; Lee, S. Y.; Kondo, R.; Adachi, C., A Six-Carbazole-Decorated Cyclophosphazene as a Host with High Triplet Energy to Realize Efficient Delayed-Fluorescence OLEDs. *Mater. Horiz*. **2014**, *1*(2), 264-269, DOI: 10.1039/C3MH00079F.

[36] Koumura, N.; Hara, K., Development of Carbazole Dyes for Efficient Molecular Photovoltaics. *J. Synth. Org. Chem. Jpn*. **2010**, *68*, 399-408, DOI: 10.5059/yukigoseikyokaishi.68.399.

[37] Wang, Z. S.; Koumura, N.; Cui, Y.; Takahashi, M.; Sekiguchi, H.; Mori, A.; Kubo, T.; Furube, A.; Hara, K., Hexylthiophene-Functionalized Carbazole Dyes for Efficient Molecular Photovoltaics: Tuning of Solar-Cell Performance by Structural Modification. *Chem. Mater*. **2008**, *20*(12), 3993-4003, DOI: 10.1021/cm8003276.

[38] Haid, S.; Mishra, A.; Uhrich, C.; Pfeiffer, M.; Bäuerle, P., Dicyanovinylene-Substituted Selenophene–Thiophene Co-Oligomers for Small-Molecule Organic Solar Cells. *Chem. Mater*. **2011**, *23*(20), 4435-4444, DOI: 10.1021/cm201392c.

[39] Haid, S.; Mishra, A.; Weil, M.; Uhrich, C.; Pfeiffer, M.; Bäuerle, P., Synthesis and Structure-Property Correlations of Dicyanovinyl-Substituted Oligoselenophenes and Their Application in Organic Solar Cells. *Adv. Funct. Mater*. **2012**, *22*(20), 4322-4333, DOI: 10.1002/adfm.201201018.

[40] Hossein Habibi, A.; Josse, P.; Marqués, P. S.; Blanchard, P.; Cabanetos, C., Effect of Chalcogen Incorporation and Rigidification on the Photovoltaic Properties of Simple Arylamine-Based D-π-A Push-Pull Molecular Systems. *ChemPhotoChem*. **2022**, *6*(10), e202200114, DOI: 10.1002/cptc.202200114

[41] Civalleri, B.; Zicovich-Wilson, C. M.; Valenzano, L.; Ugliengo, P., B3LYP augmented with an empirical dispersion term (B3LYP-D*) as applied to molecular crystals. *CrystEngComm* **2008**, *10*(4), 405-410, DOI: 10.1039/B715018K.

[42] Yanai, T.; Tew, D. P.; Handy, N. C., A new hybrid exchange-correlation functional using the Coulomb-attenuating method (CAM-B3LYP). *Chem. Phys. Lett.* **2004**, *393*(1-3), 51-57, DOI: 10.1016/j.cplett.2004.06.011.

[43] Becke, A. D., Density-functional thermochemistry. I. The effect of the exchange-only gradient correction. *J. Chem. Phys.* **1992**, *96*(3), 2155-2160, DOI: 10.1063/1.462066.

[44] Chai, J. -D.; Head-Gordon, M., Long-range corrected hybrid density functionals with damped atom–atom dispersion corrections. *Phys. Chem. Chem. Phys.* **2008**, *10*(44), 6615-6620, DOI: 10.1039/B810189B.

[45] Adamo, C.; Barone, V., Exchange functionals with improved long-range behavior and adiabatic connection methods without adjustable parameters: The mPW and mPW1PW models. *J. Chem. Phys.* **1998**, *108*(2), 664-675, DOI: 10.1063/1.475428.

[46] Mennucci, B.; Tomasi, J.; Cammi, R.; Cheeseman, J. R.; Frisch, M. J.; Devlin, F. J.; Stephens, P. J., Polarizable continuum model (PCM) calculations of solvent effects on optical rotations of chiral molecules. *J. Phys. Chem. A* **2002**, *106* (25), 6102-6113, DOI: 10.1021/jp020124t.

[47] Frisch, M. J.; Trucks, G. W.; Schlegel, H. B.; Scuseria, G. E.; Robb, M. A.; Cheeseman, J. R.; Scalmani, G.; Barone, V.; Mennucci, B.; Petersson, G. A.; *et al*., Gaussian09, Revision A. *Gaussian Inc.* Wallingford, CT, **2009**, *121*, 150-166.

[48] Yang, S. Y.; Kan, Y. H.; Yang, G. C.; Su, Z. M.; Zhao, L., TD-DFT investigation on the low-lying excited states of spiro-bithiophene. *Chem. Phys. Lett.* **2006**, *429*(1-3), 180-184, DOI: 10.1016/j.cplett.2006.07.078.

[49] EL Ouafy, H.; Aamor, M.; Oubenali, M.; Mbarki, M.; Gamouh, A.; EL Haimouti, A.; EL Ouafy, T., 4-Bromo-N, N-dimethylaniline, 4-fluoro-N, N-dimethylaniline, 4-methyl-N, N-dimethylaniline: Density-functional theory study. *Sci. Eng. Health Stud*. **2021**, 21020012-21020012, DOI: 10.14456/sehs.2021.39.

[50] EL Ouafy, H.; EL Ouafy, T.; Oubenali, M.; EL Haimouti, A.; Gamouh, A.; Mbarki, M., Analysis of the Chemical Reactivity of Limonene by the Functional Density Theory Method Using Global Descriptors. *J. Chem. Health Risks*. **2021**, *11*(2), 213-221, DOI: 10.22034/jchr.2021.1910282.1189.

[51] EL Ouafy, H.; Aamor, M.; Amini, L.; Oubenali, M.; Mbarki, M.; Haimouti, A.; EL Ouafy, T., Molecular

docking, spectroscopic studies and simulation of the dopamine molecule by the DFT and MP2 methods. *Curr. Chem. Lett*. **2022**, *11*(3), 291-298, DOI: 10.5267/j.ccl.2022.3.005

[52] EL Ouafy, H.; Aamor, M.; Oubenali, M.; Mbarki, M.; EL Haimouti, A.; EL Ouafy, T., Molecular Structure, Electrostatic Potential and HOMO, LUMO Studies of 4-Aminoaniline, 4-Nitroaniline and 4-Isopropylaniline by DFT. *Sci. Technol. Asia*. **2022**, 9-19., DOI: 10.14456/scitechasia.2022.2.

[53] EL Ouafy, H.; Aamor, M.; Oubenali, M.; Mbarki, M.; EL Haimouti, A.; EL Ouafy, T., Theoretical study of the stability and reactivity of salicylic acid isomers by the DFT method. *Curr. Chem. Lett.* **2022**, *11*, 183-190, DOI: 10.5267/j.ccl.2022.2.002.

[54] Aamor, M.; EL Ouafy, H.; Halil, L.; Boutkbout Nait Moudou, M.; Chriyaa, M. R.; Iken, W.; Naciri, S.; EL Ouafy, T., Spectroscopic analysis and theoretical comparison of the reactivity of 6-amino-3(R)benzophenone reactions with acetylacetone. *Chem. Rev. Lett.* **2024**, 7, 942-956, DOI: 10.22034/crl.2024.463313.1356.

[55] Pearson, R. G., Absolute electronegativity and hardness correlated with molecular orbital theory. *Proc. Natl. Acad. Sci. U.S.A.* **1986**, *83*(22), 8440-8441, DOI: 10.1073/pnas.83.22.8440.

[56] Guillén-López, A.; Delesma, C.; Amador-Bedolla, C.; Robles, M.; Muñiz, J., Electronic structure and nonlinear optical properties of organic photovoltaic systems with potential applications on solar cell devices: a DFT approach. *Theor. Chem. Acc.* **2018**, *137*, 1-15, DOI: 10.1007/s00214-018-2267-3.

[57] Leclerc, N.; Michaud, A.; Sirois, K.; Morin, J.-F.; Leclerc, M., Synthesis of 2,7-carbazolenevinylene-based copolymers and characterization of their photovoltaic properties. *Adv. Funct. Mater.* **2006**, *16*(13), 1694-1704, DOI: 10.1002/adfm.200600171.

[58] Janjua, M. R. S. A., Theoretical understanding and role of guest π-bridges in triphenylamine-based donor materials for high-performance solar cells. *Energy Fuels* **2021**, *35*(15), 12451-12460, DOI: 10.1021/acs.energyfuels.1c01625.

[59] Wurfel, P., The Chemical Potential of Radiation. *J. Phys. C: Solid State Phys*. **1982**, *15*(18), 3967, DOI: 10.1088/0022-3719/15/18/012.

[60] Kolev, T. M.; Yancheva, D. Y.; Stamboliyska, B. A.; Dimitrov, M. D.; Wortmann, R., Nonlinear optical properties of pyridinium-betaines of squaric acid: Experimental and theoretical study. *Chem. Phys*. **2008**, *348*(1-3), 45-52, DOI: 10.1016/j.chemphys.2008.02.018

[61] Scrocco, E.; Tomasi, J., Electronic molecular structure, reactivity and intermolecular forces: an euristic interpretation by means of electrostatic molecular potentials. *Adv. Quantum Chem*. **1978**, *11*, 115-193, DOI: 10.1016/S0065-3276(08)60236-1.

[62] Luque, F. J.; López, J. M.; Orozco, M., Perspective on "Electrostatic interactions of a solute with a continuum. A direct utilization of ab initio molecular potentials for the prevision of solvent effects". *Theor. Chem. Acc*. **2000**, *103*, 343-345, DOI: 10.1007/s002149900013.

[63] Gadisa, A.; Svensson, M.; Andersson, M. R.; Inganäs, O., Correlation between oxidation potential and open-circuit voltage of composite solar cells based on blends of polythiophenes/fullerene derivative. *Appl. Phys. Lett*. **2004**, *84*(9), 1609-1611, DOI: 10.1063/1.1650878.

[64] Wang, G.; Chen, X. Y.; Qiao, F. L.; Wu, Z.; Huang, N. E., On intrinsic mode function. *Adv. Adapt. Data Anal*. **2010**, *2*(03), 277-293, DOI: 10.1142/S1793536910000549.

[65] Ding, W. L.; Wang, D. M.; Geng, Z. Y.; Zhao, X. L.; Xu, W. B., Density functional theory characterization and verification of high-performance indoline dyes with D–A–π–A architecture for dye-sensitized solar cells. *Dyes Pigm*. **2013**, *98*(1), 125-135, DOI: 10.1016/j.dyepig.2013.02.008.

[66] Zhang, J.; Kan, Y. H.; Li, H. B.; Geng, Y.; Wu, Y.; Su, Z. M., How to design proper π-spacer order of the D-π-A dyes for DSSCs? A density functional response. *Dyes Pigm*. **2012**, *95*(2), 313-321, DOI: 10.1016/j.dyepig.2012.05.020.

[67] Fan, W.; Tan, D.; Deng, W. Q., Inside Cover: Acene-Modified Triphenylamine Dyes for Dye-Sensitized Solar Cells: A Computational Study (ChemPhysChem 8/2012). *ChemPhysChem*. **2012**, *13*(8), 1966-1966, DOI: 10.1002/cphc.201290036.

[68] Zhang, J.; Li, H. B.; Sun, S. L.; Geng, Y.; Wu, Y.; Su, Z. M., (2012). Density functional theory characterization and design of high-performance diarylamine-fluorene dyes with different π spacers for dye-sensitized solar cells. *J. Mater. Chem.* **2012**, *22*(2), 568-576, DOI: 10.1039/C1JM13028E.

[69] Guo, X.; Zhou, N.; Lou, S. J.; Smith, J.; Tice, D. B.; Hennek, J. W.; Ortiz, R. P.; Navarrete, J. T. L.; Li, S.; Strzalka, J.; Chen, L. X.; Chang, R. P. H.; Facchetti, A. ; Marks, T. J., Polymer solar cells with enhanced fill factors. *Nat. Photonics*. **2013**, *7*(10), 825-833, DOI: 10.1038/nphoton.2013.207.

[70] Zhao, C.; Zhang, Q.; Zhou, K.; Ge, H.; Wang, W.; Yin, S., Theoretical Prediction on Photovoltaic Properties of 4Cl-BPPQ/PC61BM System via Density Functional Theory Calculations. *Chin. J. Chem*. **2016**, *34*(11), 1143-1150, DOI: 10.1002/cjoc.201600350.

[71] Zhang, R.; Du, B.; Sun, G.; Sun, Y., Experimental and theoretical studies on o-, m-and p-chlorobenzylideneaminoantipyrines. *Spectrochim. Acta A Mol. Biomol. Spectrosc.* **2010**, *75*(3), 1115-1124., DOI: 10.1016/j.saa.2009.12.067.

[72] Mohr, T.; Aroulmoji, V.; Ravindran, R. S.; Müller, M.; Ranjitha, S.; Rajarajan, G.; Anbarasan, P. M., DFT and TD-DFT study on geometries, electronic structures and electronic absorption of some metal free dye sensitizers for dye sensitized solar cells. *Spectrochim. Acta A Mol. Biomol. Spectrosc.* **2015**, *135*, 1066-1073, DOI: 10.1016/j.saa.2014.07.094.

[73] Xie, M.; Wang, J.; Xia, H. Q.; Bai, F. Q.; Jia, R.; Rim, J. G.; Zhang, H. X., Theoretical studies on the spectroscopic properties of porphyrin derivatives for dye-sensitized solar cell application. *RSC Adv*. **2015**, *5*(42), 33653-33665, DOI: 10.1039/C4RA17080F

[74] Senge, M. O.; Fazekas, M.; Notaras, E. G.; Blau, W. J.; Zawadzka, M.; Locos, O. B.; Ni Mhuircheartaigh, E. M., Nonlinear optical properties of porphyrins. *Adv. Mater.* **2007**, *19*(19), 2737-2774, DOI: 10.1002/ adma.200601850.